Thickness-dependent transport properties of $Nd_{2/3}Sr_{1/3}MnO_3$ thin films

A. Barman[a] and G. Koren[b]
Department of Physics, Technion–Israel Institute of Technology, Haifa 32000, Israel

(Received 13 June 2000; accepted for publication 13 July 2000)

A systematic study is reported on the thickness dependence of the electrical resistivity in thin films of the giant magnetoresistance manganite $Nd_{2/3}Sr_{1/3}MnO_3$. We observed a first-order phase transition versus thickness in these films, which is seen as a jump of about 30 K in the metal-to-insulator transition temperature (T_p) at film thickness of 50–60 nm. This phenomenon is attributed to a sudden release of strain in the film as its thickness increases. We also observed at low temperatures, 5–30 K, another transition from localized-to-metallic behavior versus film thickness, which is also related to the strain relief in the films. © *2000 American Institute of Physics.* [S0003-6951(00)03137-5]

Following the discovery of giant magnetoresistance (MR) in the manganites, they have attracted renewed interest. Their resistivity versus temperature shows a peak at the metal-to-insulator (M–I) transition temperature (T_p), which is accompanied by a ferromagnetic-to-paramagnetic (FM–PM) transition at a very close temperature T_c.[1–3] These phenomena have been explained in terms of the combined effect of double-exchange[4–6] and the Jahn–Teller (JT) distortion.[7] Among the manganite materials, the $La_xCa_{1-x}MnO_3$ (LCMO) group is the one which has been studied most extensively up until now.[8,9] This is probably due to its large magnetoresistance near room temperature, which might be important for practical applications. Although $Nd_{2/3}Sr_{1/3}MnO_3$ (NSMO) has a larger temperature coefficient of resistance [(TCR), which is defined as $1/R\ dR/dT$], its T_c is rather low.[10,11] Due to its low T_c, low-field magnetoresistance (LFMR) applications are not so attractive in this class of materials. However, its larger TCR and sharper transition versus temperature makes it a potential candidate for bolometric applications.[11]

In the present study, we focus on thin films of NSMO on (100) $SrTiO_3$ (STO) substrates. The films often have different T_c and MR compared to bulk material due to lattice and thermal mismatch between the film and the substrate.[12–15] NSMO thin films were found to grow epitaxially on $LaAlO_3$ (LAO) and on STO substrates because of their relatively good lattice match. It was also found that higher oxygenation levels of the films often leads to higher T_c.[16,17] Previously, other groups have examined strain effects in thin perovskite films by preparing them at various thicknesses in separate deposition runs.[14,18,19] However, our experience shows that maintaining identical conditions in separate runs is quite difficult. Often, even a slight change in the experimental parameters such as the actual surface temperature during deposition, the oxygen flow rate, laser fluence on the target, shape of the plume, rate of cooling, etc., can affect the results significantly and mask or smear the thickness-dependent effects. For a systematic study of these effects it is, therefore, more reliable to grow all the films of varying thickness *in situ* on the same substrate in the same deposition run, and this is what was done in the present study. We first optimized the properties of the film for a thickness of about 100 nm, and then using the same deposition conditions in the same deposition run, we prepared the various films of different thicknesses by the use of a metallic shadow mask.

The NSMO films were grown epitaxially on (100) STO substrates by pulsed-laser deposition. The target used was a standard ceramic disk of $Nd_{2/3}Sr_{1/3}MnO_3$ of 1 in. diam. A KrF excimer laser was used for the deposition at a 248 nm wavelength, 5 Hz pulse rate, and $\sim$1.5 J/cm^2 fluence on the target. This yielded a deposition rate of around 0.4–0.5 Å per pulse. The optimized growth parameters were found to be a substrate temperature of $\sim$800 °C and oxygen pressure of 250 mTorr during deposition, and a postdeposition cooling rate of 500 °C/h in 0.5 atm of oxygen pressure. This yielded a maximum T_p of $\sim$220 K for a typical film thickness of 100 nm. This value of T_p is similar to the maximum value obtained for NSMO films by other groups after annealing for a much longer time at even higher temperatures.[16,17] Thus our relatively slow cooling rate allows us to avoid the long postdeposition annealing process used by the other groups.

In order to study the effect of thickness on the electrical transport properties of these films, we have grown eight film stripes of increasing thickness on the same (100) STO wafer of 1×1 cm^2. To grow these stripes, we used a metallic shadow mask whose edge was touching the wafer at an angle of 45°. By placing this mask at seven equally spaced positions over the wafer and adding a certain deposition thickness in each position, the stripes were prepared. Since all the deposition conditions are held unchanged, we are in a position to study the thickness-dependent properties of the films. However, due to the flow pattern of the plume near the edge of the mask, the borders between consecutive film stripes are not very sharp and have small thickness gradients. Thus, in order to measure the electrical resistivity of the independent films accurately, we patterned eight microbridges on them such that the microbridges fall in the center of each film stripe. For the patterning we used a waterless PMMA resist, a deep UV mask aligner, and etching by Ar-ion beam milling at $\sim$80 K. This yielded eight microbridges of 100 μm length

[a]Present address: Department of Physics, V. S. Mahavidyalaya, P.O. Manikpara, Dist.: Midnapore, W.B., India.
[b]Electronic mail: gkoren@physics.technion.ac.il

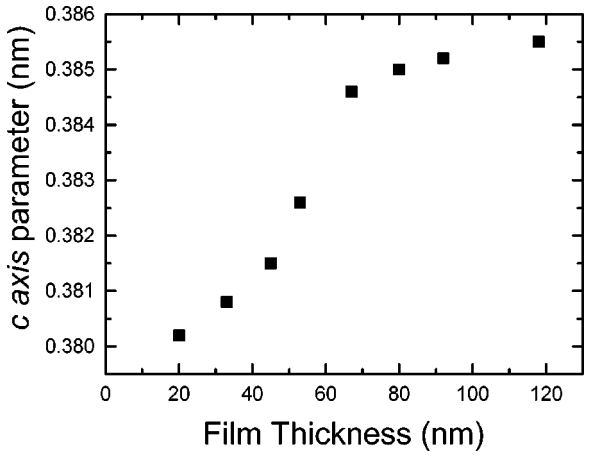

FIG. 1. *C*-axis lattice parameter as a function of film thickness.

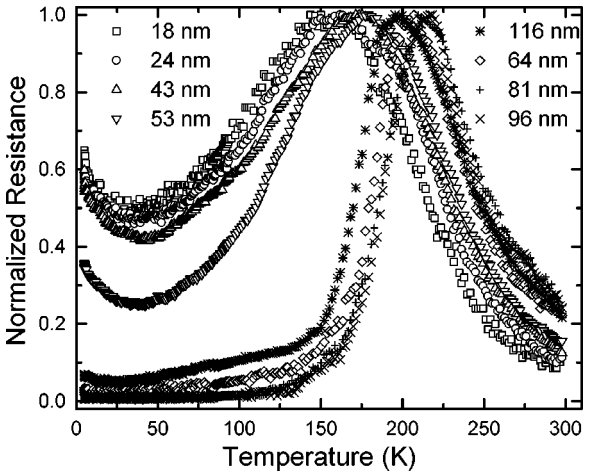

FIG. 2. Resistance of the eight films of different thicknesses normalized to their peak values (R_N) vs temperature.

and 10 μm width of the individual films. The thickness of the films was measured with the aid of an atomic-force microscope. First, the combined thickness of the films and the milling steps into the STO wafer were measured on each microbridge ($d_f + d_s$). Then, after the transport measurements were completed, the films were etched away in Aqua Rega and the milling steps into the STO substrate (d_s) were measured and subtracted from the previous measurements to yield the desired film thickness (d_f). The structure of the films was studied by normal Bragg x-ray diffraction. The electrical resistivity of all the microbridges was measured in a single cooling run from 300 to 5 K using the standard four-probe technique.

The x-ray diffraction results of our films show that each one of them is of purely single phase and oriented with its *c* axis normal to the wafer. The *c*-axis lattice parameters of the various films were obtained from the strongest reflection of the (002) peak. Figure 1 shows the pseudocubic *c*-axis lattice parameter of the different films as a function of their thickness. One can see that the lattice parameter is increasing gradually as a function of film thickness from a value of 3.800 Å for the 20-nm-thick film up to a thickness of about 50 nm. From slightly above this thickness, it increases rapidly in a small range of 10 nm to a high value of 3.848 Å, which is quite close to that of bulk NSMO. This is followed by an even weaker increase to 3.855 Å for the 120-nm-thick film. The full width at half maximum of the diffraction peaks is also seen to decrease with increasing film thickness, which indicates improved crystallinity of the thicker films. We thus conclude that for film thickness higher than 60 nm, the structure slowly approaches that of the bulk material. Bulk NSMO has a pseudocubic lattice parameter of 3.86 Å, whereas the STO has a cubic lattice parameter of 3.905 Å. The lattice mismatch between them is thus 1.16% and this should lead to a considerable strain in the epitaxial films. Since NSMO films on STO are expected to expand biaxially in the $a-b$ plane of the films, the *c*-axis lattice parameter should be compressed. Figure 1 shows that this is exactly what we observed. The *c*-axis lattice parameter increases with increasing film thickness as strain is relieved, and then saturates close to the bulk value.

Figure 2 shows the temperature dependence of the electrical resistance of the NSMO films of different thicknesses normalized to their peak values. A typical value of the absolute resistivity at the peak temperatures of the 64-, 81-, and 96-nm-thick films, whose strain is relieved to a large extent, is about $1 \pm 0.1\,\Omega$ cm. All the films show the characteristic M–I transition of this class of materials. Below the transition, the resistivity is metallic and above the transition it is insulating. The characteristic peak temperature, which corresponds to the M–I transition and the FM–PM transition generally increases with thickness. Figure 3 shows a plot of the peak temperature T_p, and the normalized resistance at 5 and 300 K as a function of the films' thickness. All these parameters change significantly with thickness, and most interestingly, they all show a drastic change around the thickness of 50–60 nm. T_p increases rapidly from 178 to 207 K, by almost 30 K following a thickness variation of only 11 nm. Since this is also accompanied by a similar sharp increase in the *c*-axis parameter (see Fig. 1), we consider this behavior as due to a first-order phase transition induced by the strain relief in the film. Above 60 nm, T_p increases slowly again and reaches a maximum around 220 K. Moreover, Fig. 3 shows that even far away from the peaks' temperature at 5 and 300 K, the normalized resistance is still affected by this phase transition and shows a large variation around the critical thickness of 50–60 nm. The film of maximum thickness, however, shows a different behavior from this trend, and this

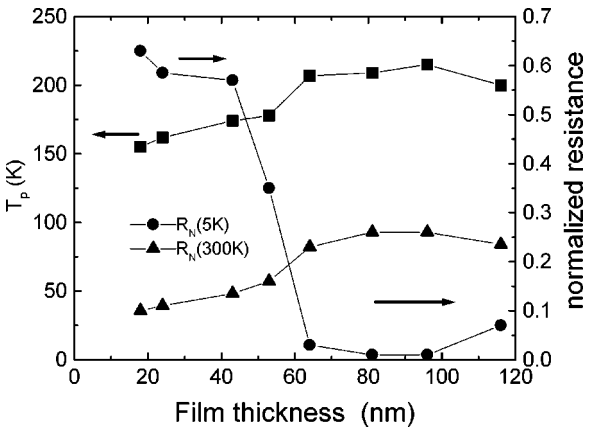

FIG. 3. M–I transition temperature T_p, R_N(5 K) and R_N(300 K) as a function of film thickness.

may result from its location near the edge of the wafer, which may produce extra strain in this film that reduces its T_p. Another interesting observation comes from the low- and high-temperature resistivity behaviors of these samples (see Fig. 2). In the low-temperature region, the films with thickness below the threshold thickness of 50–60 nm show an upturn in the resistivity, which indicates the existence of localized states in these films. In the thicker films, however, with thickness above 60 nm, a flat resistivity versus temperature is seen which implies that these films are on the border of being metallic. At high temperatures well above T_p, all films show insulating behavior.

Since strain is so important in the phenomena observed, we focus on it now. The resistivity of the manganites and T_p are well studied as a function of external hydrostatic pressure,[20] and internal chemical pressure[21,22] exerted by replacing the *A*-site cations by larger or smaller cations. While increase of internal pressure generally leads to a smaller T_c and T_p, the external hydrostatic pressure has the opposite effect. This was explained as resulting from a distortion of the MnO_6 octahedra, which leads to a change in the Mn^{3+}–O–Mn^{4+} bond angle. This weakens the double-exchange interaction, leads to a variation in the width of the electronic bands, and therefore, affects T_c.[20,22] In the thin-film case, the strain is induced by the substrate, and this is analogous to the application of an *external* pressure which produces a considerable change in the resistivity and T_c. Recently, Wang *et al.*[14] studied the thickness dependence of T_c in PrSrMO films grown on various wafers. In order to explain their result they used the theory given by Millis and co-workers[23] who considered two kinds of strain, one is the symmetry conserving (uniform) bulk strain ϵ_B, and the other is the symmetry breaking Jahn–Teller strain ϵ^*. T_c of the strained film is thus given by[14]

$$T_c(\epsilon)=T_c(\epsilon=0)[1-\alpha\epsilon_B-0.5\Delta\epsilon^{*2}], \quad (1)$$

where $T_c(\epsilon=0)$ is T_c in the unstrained film, and α and Δ are the corresponding strain coefficients $1/T_c dT_c/d\epsilon_B$ and $1/T_c dT_c/d\epsilon^*$, respectively. The second term in Eq. (1) can be either positive or negative depending on the sign of strain. In our NSMO/STO films, there is a tensile strain in the film plane, which causes some compression along the normal to the film plane, and as a result ϵ_B should be positive. This gives a negative contribution from the second term since α is positive (see Fig. 3). The third term is related to the electron localization due to the JT effect and is always negative. Thus, both terms reduce T_c with increasing strain, as we actually observed in Fig. 3 (note that T_c and T_p are nearly equal here). Interestingly, films below the threshold thickness for strain relief show a strong localization effect in the low-temperature range. This is likely to be present throughout the temperature range, whereas for the films of higher thickness the localization effect is rather smaller and not even seen in the low-temperature range. So, in the lower thickness regime both the bulk strain and the JT effect are quite high and reduce T_p considerably. In the higher thickness regime, however, the bulk strain becomes quite low as the lattice parameter of the film approaches very closely the bulk value. In addition, the localization becomes less pronounced and, hence, T_p is enhanced and approaching the bulk material value. Thus the sudden transition of T_p and the transition of the low-temperature resistivity behavior from a strongly localized state to an almost nonlocalized state seem to be two correlated phenomena which originate in the sudden relief of strain in the lattice.

In conclusion, we found a first-order phase transition of T_p in NSMO films at 50–60 nm thickness, which is closely related to a sudden relief of strain in the films. The same strain relief mechanism is also responsible for a transition of the low-temperature resistivity from localized-to-metallic behavior with increasing film thickness.

This research was supported in part by the Israel Science Foundation, the Heinrich Hertz Minerva Center for high-temperature superconductivity, and the Fund for the Promotion of Research at the Technion.

[1] R. von Helmolt, J. Wecker, B. Holzapfel, L. Schultz, and K. Samwer, Phys. Rev. Lett. **71**, 2331 (1993).
[2] S. Jin, T. H. Tiefel, M. McCormack, R. A. Fastnacht, R. Ramesh, and L. H. Chen, Science **264**, 413 (1994).
[3] A. P. Ramirez, J. Phys.: Condens. Matter **9**, 8171 (1996).
[4] C. Zener, Phys. Rev. **82**, 403 (1951).
[5] P. W. Anderson and H. Hasegawa, Phys. Rev. **100**, 675 (1955).
[6] P. G. de Gennes, Phys. Rev. **118**, 141 (1960).
[7] A. J. Millis, B. I. Shraiman, and R. Mueller, Phys. Rev. Lett. **77**, 175 (1996).
[8] P. Schiffer, A. P. Ramirez, W. Bao, and S.-W. Cheong, Phys. Rev. Lett. **75**, 3336 (1995).
[9] G.-Q. Gong, C. L. Canedy, G. Xiao, J. Z. Sun, A. Gupta, and W. J. Gallagher, Appl. Phys. Lett. **67**, 1783 (1995); G.-Q. Gong, A. Gupta, G. Xiao, P. Lecoeur, and T. R. McGuire, Phys. Rev. B **54**, R3742 (1996).
[10] G. C. Xiong, Q. Li, H. L. Ju, S. N. Mao, L. Senapathi, X. X. Xi, R. L. Greene, and T. Venkatesan, Appl. Phys. Lett. **66**, 1427 (1995).
[11] A. Goyal, M. Rajeswari, R. Shreekala, S. E. Lofland, S. M. Bhagat, T. Boettcher, C. Kwon, R. Ramesh, and T. Venkatesan, Appl. Phys. Lett. **71**, 2535 (1997).
[12] H. S. Wang and Q. Li, Appl. Phys. Lett. **73**, 2360 (1998).
[13] T. K. Nath, R. A. Rao, D. Lavric, C. B. Eom, L. Wu, and F. Tsui, Appl. Phys. Lett. **74**, 1615 (1999).
[14] H. S. Wang, E. Wertz, Y. F. Hu, Q. Li, and D. G. Schlom, J. Appl. Phys. **87**, 7409 (2000).
[15] K. Steenbeck and R. Hiergeist, Appl. Phys. Lett. **75**, 1778 (1999).
[16] G. C. Xiong, Q. Li, H. L. Ju, R. L. Greene, and T. Venkatesan, Appl. Phys. Lett. **66**, 1689 (1995).
[17] M. Rajeswari, R. Shreekala, A. Goyal, S. E. Lofland, S. M. Bhagat, K. Ghosh, R. P. Sharma, R. L. Greene, R. Ramesh, and T. Venkatesan, Appl. Phys. Lett. **73**, 2672 (1998).
[18] J. Z. Sun, D. W. Abraham, R. A. Rao, and C. B. Eom, Appl. Phys. Lett. **74**, 3017 (1999).
[19] W. Prellier, A. Biswas, M. Rajeswari, T. Venkatesan, and R. L. Grene, Appl. Phys. Lett. **75**, 397 (1999).
[20] Y. Moritomo, A. Asamitsu, and Y. Tokura, Phys. Rev. B **51**, 16491 (1995).
[21] H. Y. Hwang, S.-W. Choeng, R. G. Radaelli, M. Marezio, and B. Batlogg, Phys. Rev. Lett. **75**, 914 (1995).
[22] A. Barman, M. Ghosh, S. Biswas, S. K. De, and S. Chatterjee, Solid State Commun. **106**, 691 (1998).
[23] A. J. Millis, T. Darling, and A. Migliori, J. Appl. Phys. **83**, 1588 (1998); A. J. Millis, A. Goyal, M. Rajeswari, K. Ghosh, R. Shreekala, R. L. Greene, R. Ramesh, and T. Venkatesan (unpublished).